Piezotronic Effect on the Transport Properties of GaN Nanobelts for Active Flexible Electronics

Ruomeng Yu, Lin Dong, Caofeng Pan, Simiao Niu, Hongfei Liu, Wei Liu, Soojin Chua, Dongzhi Chi, and Zhong Lin Wang*

GaN, a direct wide bandgap semiconductor with key application in light-emitting diodes, [1] has attracted a wide range of interest in science and technology. Quasi-one-dimensional GaN nanostructures such as nanowires (NWs) and nanobelts (NBs) are considered as important building blocks for fabricating various nanodevices. In analogous to ZnO, GaN has the wurtzite structure and great piezoelectric characteristics, but with a much better chemical stability than ZnO in atmosphere and/or under acid conditions. A piezoelectric potential (piezopotential) is created in GaN by applying a stress. The piezotronic effect is well studied in ZnO for nanogenerators (NG),[2,3] hybrid NG,[4] piezoelectric field effect transistors (FET),[5,6] piezoelectric diodes,[7] and piezoelectric chemical sensors.[8] NGs have already been fabricated using GaN nanowires.[9] Here, we study the piezotronic effect on devices fabricated using GaN NBs. Our results show that the piezotronic effect can significantly tune the Schottky barrier heights (SBH) at the two contacts under externally applied strains. A theoretical model is proposed to explain the observed electromechanical behaviors.

GaN NBs were fabricated via the method called strain-controlled cracking of thin solid films.[10] **Figure 1**a shows typical scanning electron microscopy (SEM) images of as-fabricated GaN NBs, which can be seen clearly that the NBs are well separated, straight and parallel with each other, with lengths of several hundred micrometers and widths of 10 μm, the inset
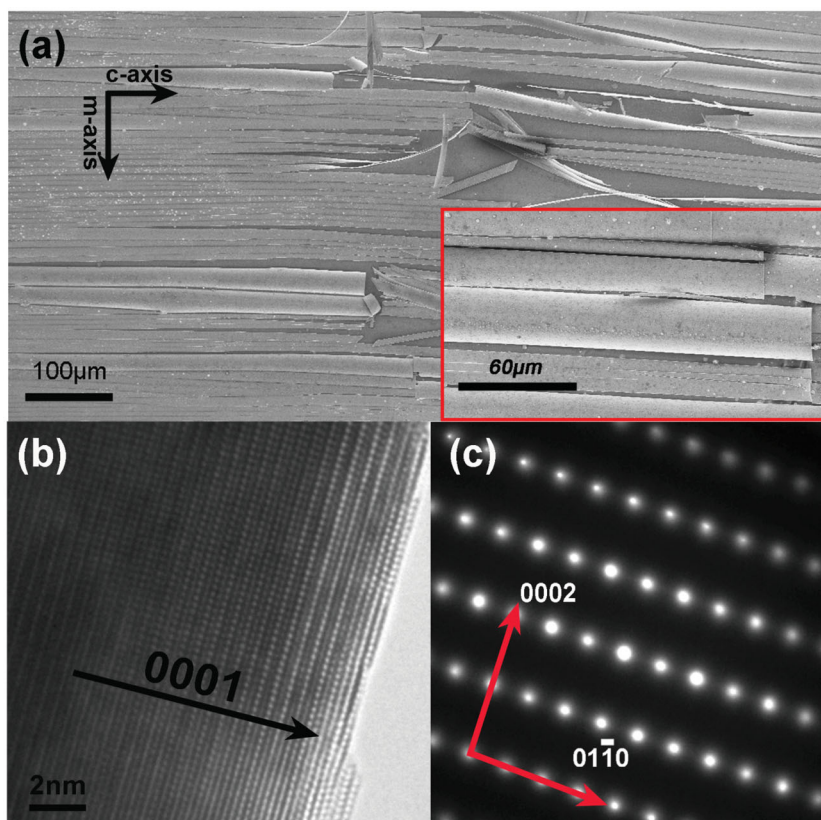

Figure 1. a) SEM image of GaN NBs. The inset is a high-magnification SEM image, showing details of the GaN belt. b) HRTEM image of a GaN NB, indicating that the GaN belt is single crystal and grown along *c*-axis. c) Corresponding SAED pattern of the same GaN NB in (b).

of Figure 1a is a high-magnification SEM image, showing details of the n-type GaN belts. A high-resolution transmission electron microscopy (HRTEM) image and the corresponding

R. M. Yu, Dr. L. Dong, Dr. C. F. Pan, S. M. Niu,
Prof. Z. L. Wang
School of Materials Science and Engineering
Georgia Institute of Technology
Atlanta, GA 30332-0245, USA
E-mail: zhong.wang@mse.gatech.edu
Dr. L. Dong
School of Materials Science and Enginnering
Zhengzhou University
Zhengzhou, 450001, China

Prof. Z. L. Wang
Beijing Institute of Nanoenergy and Nanosystems
Chinese Academy of Sciences, Beijing, China
Prof. H. F. Liu, Prof. S. Chua, Dr. D. Z. Chi
Institute of Materials Research and Engineering
A∗STAR (Agency for Science, Technology and Research)
Singapore 117602, Singapore
Dr. W. Liu
School of Electrical and Electronic Engineering
Luminous! Center of Excellence for Semiconductor Lighting and Display
Nanyang Technology University
Singapore 639798, Singapore

select area electron diffraction (SAED) taken from the end of a GaN NB are presented in Figure 1b,c, indicating that the GaN belt is a single crystal with length direction of *c*-axis, surface normal plane of (–2110) and side surfaces (01–10).

The device was fabricated by transferring and bonding an individual GaN NB laterally on the substrate, like polystyrene (PS) film, with its *c*-axis in the plane of the substrate pointing to the source. Silver paste was used to fix the two ends of the NB, serving as source and drain electrodes, respectively. For such a Ag-GaN NB-Ag device, it could be treated as a metal-semiconductor-metal (M-S-M) structure. A thin layer of polydimethylsiloxane (PDMS) was used to package the device. This PDMS thin layer can not only enhance the adhesion of the silver paste to the PS substrate, but can also prevent the GaN NB from contamination or corrosion by gases or liquid. Finally, a flexible, optically transparent, and well-packaged piezotronic device was fabricated. The schematic of the measurement set-up for studying the piezotronic effect on GaN NB device is presented in **Figure 2**a. One end of the PS substrate was fixed tightly on a sample holder, with the other end free to be bent. A three-dimensional (3D) mechanical stage with movement resolution of 1 μm was used to apply the strain on the free end of the PS substrate. A typical optical image of the as-fabricated GaN NB device is presented in Figure 2a.

Current–time (*I*–*t*) characteristics of the devices at different strains were recorded to investigate the piezotronic effect on GaN NB devices when compressive strains were applied to and released from the GaN NB device with the bias voltage being fixed at 3 V. The compressive strain applied to the device was increased step by step from –0.7%, –1.1% to –1.3% and then decreased step by step back to –0.7%. The corresponding current of the GaN NB device increased step by step as well first from 1.4 μA to 7.8 μA, and then fell back to 1.4 μA, with a peak value at the strain of –1.3%. Five more repeated tests were carried out on the same device to show the reproducibility and stability of the device. Due to the space limitation, only two of six results are presented in Figure 2c,d. The current reached almost the same value under the same strains in the two tests and the current can fully recover when the strain was released. The average currents of the device under different strains at a bias of 3 V were extracted from three trials and plotted in Figure 2b; they show the good reproducibility and stability of the GaN NB device.

The piezotronic effect on GaN NBs was examined and typical current–voltage (*I*–*V*) curves of these GaN NB devices under different strains are shown in **Figure 3**a,b, which are obviously asymmetric. The insets in Figure 3a,b are corresponding schematic diagrams of configurations of GaN NB devices under different strains. To be more clear, the current value at a fixed bias under different strains was extracted from Figure 3a,b,
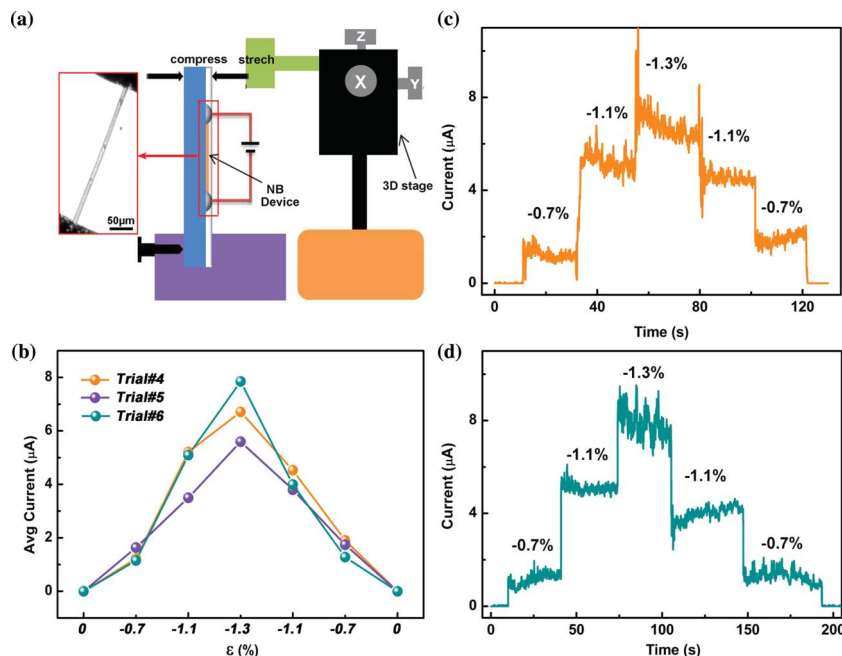

Figure 2. Reproducibility on the current response of the GaN NB device under different compressive strains. a) Schematic of the measurement setups for studying the piezotronic effect in GaN NB, the inset is an optical image of a typical GaN NB device. b) Plots of the average current responses vs. the applied strain. The data were extracted from (c,d), showing a good reproducibility of the GaN NB device. All the data in (b–d) are obtained from the same device. c,d) Current response of a GaN NB device under different compressive strains when the bias voltage was fixed at 3 V. The compressive strain applied on the device increased step by step from –0.7%, –1.1% to –1.3% and then fell back to –0.7%. The corresponding current of the GaN NB device increased first step-by-step and then decreased, with a peak value at a strain of –1.3%.

plotted at most right side correspondingly, which shows clearly that compressive strain leads to a monotone increasing current (Figure 3a) and tensile strain leads to a monotone decreasing current (Figure 3b).

These *I*–*V* characteristics clearly demonstrate that there were Schottky barriers presenting at the two GaN/Ag contacts but with distinctly different barrier heights.[11,12] These Schottky barriers at the metal/semiconductor interfaces play a crucial role in determining the electrical transport property of the M-S-M structure. It is important to quantitatively fit the *I*–*V* curve in order to determine the nature of the electric transport across the M-S-M structure.[11] The fitting of the *I*–*V* characteristics of the GaN NB under different strains was carried out using a GUI program PKUMSM developed by Peng et al.,[13] which uses the following theoretical model.

When the device is supplied with a bias *V* over the two electrodes, the voltage *V* is distributed on the Schottky barriers and the unexhausted part of the GaN NB, denoted here by V_1, V_2, V_{NB} respectively, i.e.,

$$V = V_1 + V_2 + V_{NB} \qquad (1)$$

The current–voltage relationships of the three components, i.e., the reverse biased Schokkty barrier ($I_1 – V_1$), the NB ($I_{NB} – V_{NB}$) and the forward biased Schottky barrier ($I_2 – V_2$) are given by
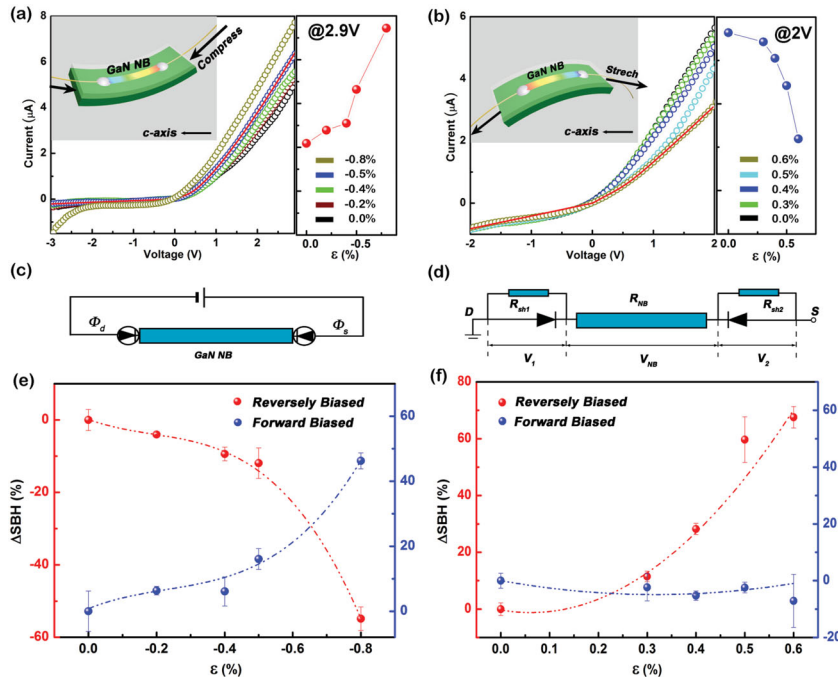
$$I_1 = S_1 J_r (V_1) + V_1/R_{sh1} \qquad (2)$$

Figure 3. I–V curves of the GaN NB devices when they are compressed (a) or stretched (b) to different degrees of strain, with the c-axis of GaN NB parallel to the longitudinal axis of the PS substrate. The colored lines are experimental data and the red lines are theoretical fitting. The plots of current vs. strain at a fixed bias are also presented. The current increased with increasing the strain (a), noted as SU; decreased with increasing the strain (b), noted as SD. The insets are corresponding schematic diagrams of configurations of GaN NB devices under different strains. c) Schematic of proposed sandwich model of MSM structure and d) its equivalent circuit. e,f) Relative changes of the forward and reversely biased Schottky barrier height (ΔSBH) vs. the applied strain. ΔSBH data were extracted from the theoretical simulations corresponding to a) SU and b) SD.

$$I_2 = S_2 J_f(V_2) + V_2/R_{sh2} \tag{3}$$

$$I_{NB} = V_{NB}/R_{NB} \tag{4}$$

where R_{sh1} and R_{sh2} are the shunt resistances associated with the two Schottky barriers, S_1 and S_2 are the corresponding contact areas of the two metal-semiconductor junctions respectively. $J_r(V_1)$ is the current density passing through the reverse biased Schottky barrier, and $J_f(V_2)$ is that through the forward biased Schottky barrier. For moderate bias, V is larger than $3kT/q$, i.e., 75 mV at room temperature, these current densities are given by

$$J_r(V_1) = \frac{A^* T \sqrt{\pi E_{00}}}{k} \left\{ q(V_1 - \xi) + \frac{q\phi_1}{\cosh^2(E_{00}/kT)} \right\}^{1/2}$$
$$\times \exp\left(-\frac{q\phi_1}{E_0}\right) \exp\left[q V_1 \left(\frac{1}{kT} - \frac{1}{E_0}\right)\right] \tag{5}$$

and

$$J_f(V_2) = A^* T^2 \exp\left(-\frac{q\phi_2}{kT}\right)$$
$$\times \exp\left(\frac{q V_2}{nkT}\right) \left[1 - \exp\frac{q V_2}{kT}\right] \tag{6}$$

in which ϕ_1 and ϕ_2 are the effective height of the two Schottky barriers respectively, n is an ideality factor describing the deviation of the Schottky barrier (for an ideal barrier $n = 1$), ξ is the distance between the Fermi level to the bottom of the conduction band for n-type NBs or to the top of the valence band for p-type NBs, T is temperature, $A^* = 4\pi m^* q k^2/h^3$ is the Richardson constant of the GaN NB, m^* is the effective mass of major carrier, q is the magnitude of electron charge, and k is the Boltzmann constant. It should be noted that the Schottky barrier is not a constant during measurement. This quantity depends on the applied bias and may be affected by effects such as the image force; all these effects have been included in the present model by regarding it to be an effective barrier. The two important constants are given by

$$E_0 = E_{00} \coth\left(\frac{E_{00}}{kT}\right) \tag{7}$$

and

$$E_{00} = \frac{\hbar q}{2}\left[\frac{N_d}{m^* \varepsilon_s \varepsilon_0}\right]^{1/2} \tag{8}$$

where N_d is the doping concentration, ε_s is the relative permittivity of the semiconducting NB and ε_0 is the permittivity of free space.

The current flowing through each part of the M-S-M structure is the same for a steady current so that

$$I_1 = I_2 = I_{NB} \tag{9}$$

We may rearrange the above equations into a set of two equations

$$S_1 J_r(V_1) + V_1/R_{sh1} = (V - V_1 - V_2)/R_{NS}$$
$$S_2 J_f(V_2) + V_2/R_{sh2} = (V - V_1 - V_2)/R_{NS} \tag{10}$$

Once solving this set of equations for any given bias V, we can obtain the voltage distributions V_1, V_{NB}, and V_2, the current density I passing through the M-S-M system and all the related parameters including ϕ_1 and ϕ_2 by fitting the experimental data.

Our device is considered as a single GaN NB sandwiched between two opposite Schottky barriers,[14] and an equivalent circuit is shown in Figure 3c,d. The fitting results were plotted as red lines in Figure 3a,b, together with the experimental data. It is clear that the fitting curves agree well with the experimental I–V curves in each case. Furthermore, the relative change of forward and reversely biased Schottky barrier heights (ΔSBH) of each device, corresponding to Figure 3a,b, without and under different strains were obtained and presented in Figure 3e,f. Apparently, the trends shown in Figure 3e,f of forward biased SBH and reversely biased SBH turn out to be opposite to each

other, which means that the change in barrier height was caused by the piezoelectric polarization charges at the two ends of the nanobelt. It has been reported that the SBHs of GaN Schottky barrier[15] shift under strain are attributed to a combination of band structure and piezoelectric effect.[15,16] The piezotronic effect is a polarized effect using the piezopotential as a "gate" voltage to tune/control charge carrier transport at a contact or junction within the GaN NB,[6,17] while the piezoresistive effect and parasitic capacitance effect are both non-polar effects on the electric transport;[18] therefore, the electromechanical behaviors of our GaN NB devices were dominated by the piezotronic effect.

We found that the configurations of how the NBs being placed on the substrate plays a very important role in the shape of the I–V characteristic curves. For a device with the c-axis of GaN NB parallel to the longitudinal axis of the substrate, monotone increasing (Figure 3a, noted as SU) and decreasing (Figure 3b, noted as SD) I–V curves were received when it was subjected to a compressive or tensile strain, respectively. For a device with the c-axis of the GaN NB slightly off aligning with the longitudinal axis of the substrate, more complicated I–V characteristics were obtained when it was subjected to a strain, as shown in **Figure 4**a,b. Under an increasing compressive strain, the current increased first and then decreased (Figure 4a, noted as U&D); under an increasing tensile strain, the current decreased first and then increased (Figure 4b, noted as D&U). Current value at fixed bias was extracted from Figure 4a,b and plotted on the right sides to give a clearer view on how it performed under different strains. Furthermore, the fitting results were presented as red lines in Figure 4a,b, which coincide with the experimental data very well. The corresponding plots of relative change of SBH vs. strains before and after applying strains are presented in Figure 4c,d. In each case, the reversely biased SBH and forward biased SBH changed with opposite trends as a function of strain, which once again confirms the domination of piezotronic effect to the electromechanical behaviors of these GaN NB devices.

To be sure that the configurations in which the NBs were placed on the substrate can lead to different I–V curves (i.e., for a device with c-axis of GaN NB parallel to the longitudinal axis of PS substrate, I–V curves of SU and SD types were obtained; for a device with c-axis of GaN NB slightly off alignment with the longitudinal axis of PS substrate, I–V curves of U&D and D&U types were obtained), further investigations were carried out. The I–V curves of 24 devices were studied and classified into four types: SU (Figure 3a); SD (Figure 3b); U&D (Figure 4a); D&U (Figure 4b). Among the 24 devices studied, 5 were tensile strained, among which 2 were of SD type, 2 were of D&U type, 1 was SU type; 19 of the 24 devices were compressively strained, among which 3 were of SD type, 2 were of D&U type, 9 were of SU type, and 5 were U&D type. The results are summarized in **Table 1**.
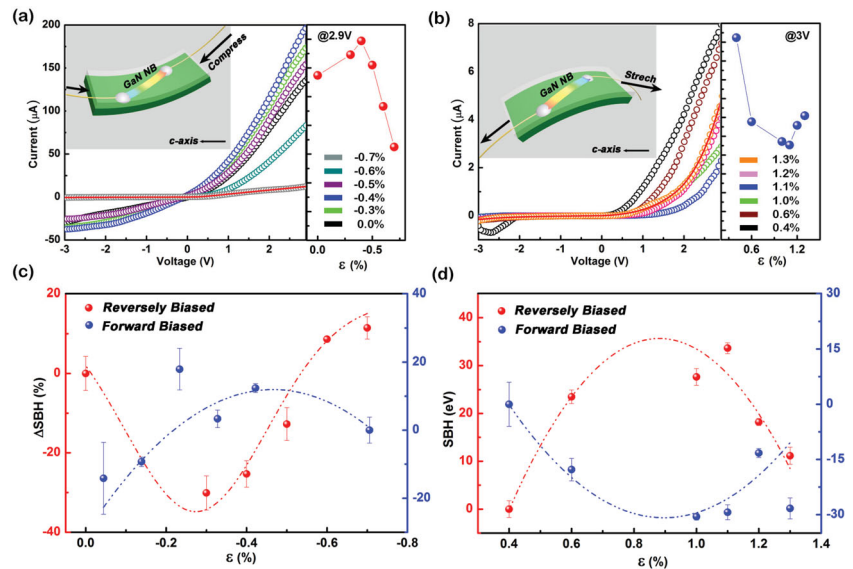

Figure 4. I–V curves of the GaN NB devices when they are compressed (a) or stretched (b) to different degrees of strain, with the c-axis of GaN NB off the longitudinal axis of the PS substrate. The colorfed lines are experimental data while the red lines are theoretical fitting. The plots of current vs. strain at fixed bias are also presented. The current increased first with increasing the strain, then decreased (a), noted as UD decreased first then increased (b), noted as D&U. The insets are the corresponding schematic diagrams of configurations of GaN NB devices under different strains. c-d) Relative changes of the forward and reversely biased Schottky barrier height (ΔSBH) vs. the applied strain. The ΔSBH data were extracted from the theoretical simulations corresponding to a) U&D and b) D&U.

Table 1. Statistics for the current response vs. the applied strain.

	Tensile	Compressive	Total
SU	1	9	10
U&D	0	5	5
SD	2	3	5
D&U	2	2	4

24 I–V curves were experimentally measured to examine the electromechanical behaviors of the GaN NB devices. 5 of the 24 devices were tensile strained, among which 2 were of SD type, 2 were of D&U type, 1 was SU type. 19 of the 24 devices were compressively strained, among which 3 were of SD type, 2 were of D&U type, 9 were of SU type, and 5 were U&D type.

A theoretical model is proposed to explain the piezotronic effect on the electrical characterization, especially the SBH of the GaN NB using the energy band diagram, as shown in **Figure 5**a–c. For piezoelectric semiconductors such as ZnO and GaN, a piezoelectric potential is created inside the NB by applying a strain/pressure/force owing to the non-central symmetric crystal structure.[2] Once a strain is created in GaN NB, a piezopotential distribution exists along the c-axis, with polarity that depending on the sign of the strain,[17] as shown in Figure 5b,c, respectively. A negative piezopotential at the semiconductor side effectively increases the local SBH, while a positive piezopotential reduces the barrier height. The role played by the piezopotential is to effectively change the local contact characteristics through an internal field depending on the crystallographic orientation of the material and the sign of the strain,[19] thus, the charge carrier transport process is tuned
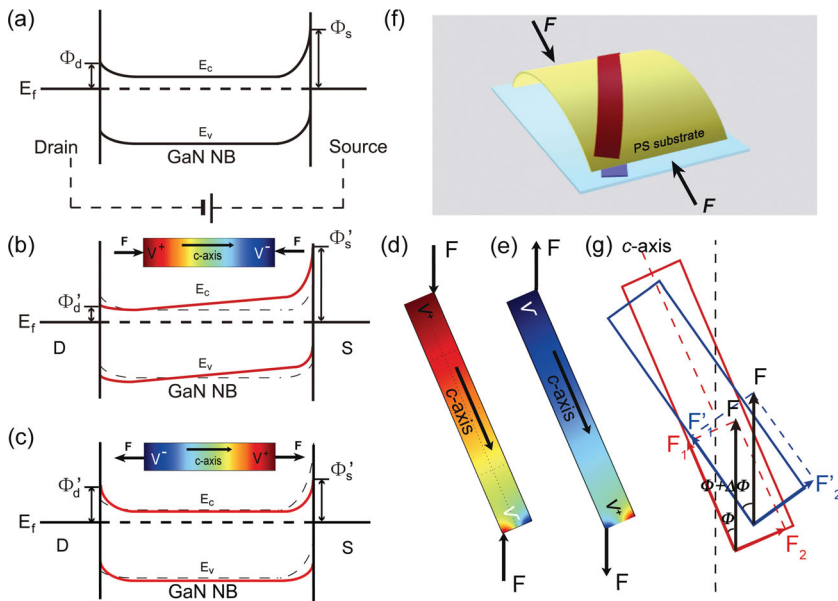
Figure 5. Schematic energy band diagrams illustrating the asymmetric Schottky barriers at the source and drain contacts of a) unstrained, b) compressively strained, and c) and tensile strained GaN NB devices. The insets of (c,d) are numerically calculated piezopotential distributions along GaN NB with its *c*-axis parallel to the longitudinal axis of the PS substrate. d,e) Numerically calculated piezopotential distributions along GaN NB with its *c*-axis aligned 30° off the longitudinal axis of the PS substrate, under compressive and tensile strain, respectively. f) 3D schematic diagram illustrating the transverse twist of an off-axis compressed GaN NB, the twist is quite obvious. g) A 2D projection of the GaN NB device showing the transverse twist of the GaN nanobelt during the compressive deformation. There is a maximum effective force exerted on the GaN NB as the external force increases, which is in accordance with the *I–V* behavior of the GaN NB devices shown in Figure 4.

at the metal-semiconductor (M-S) contact. When the GaN NB device is under compressive strain, as shown in Figure 5b, the drain has a positive potential leading to a lower SBH. Alternatively, by changing the compressive strain to tensile, as shown in Figure 5c, the drain this time has a negative potential along with a higher SBH.

For devices with GaN NB lying along the longitudinal axis of the substrate, which have SU and SD type *I–V* characteristics, when compressed with *c*-axis pointing to the source (Figure 5b), SBH at the drain will be lowered and then presents a SU type *I–V* curve. Similarly, if everything remains the same except for applying a tensile strain instead of a compressive one, SBH at the drain will be increased and gives out a SD type *I–V* curve. For devices with the *c*-axis of GaN NB lying off the longitudinal axis of PS substrate, which have U&D and D&U type *I–V* characteristics, the numerically calculated piezopotential distributions along the GaN NB when it was subjected to a 30° off-axis compressive and tensile strain are presented in Figure 5d,e, respectively. It can be seen that piezopotential distributions here are similar to that of the GaN NB lying along the longitudinal axis of the substrate, as shown in Figure 5b,c. Therefore, the configuration of GaN NB device with its *c*-axis slightly off alignment with the longitudinal axis of PS substrate is essential to U&D and D&U type *I–V* curves. From Figure 5f, it is obvious to see with such a configuration, once the device is compressed or stretched, a transverse twist is possible. Figure 5g shows a 2D projection of the GaN NB device, making it much easier and

clearer to see the twist of the GaN nanobelt during the compressive/tensile deformation. For an off-axis GaN NB device, the force applied on the substrate, denoted as F, can be divided into two components: one is parallel to the *c*-axis of the GaN NB, denoted as F_1 in Figure 5g, the other is perpendicular to the *c*-axis, denoted as F_2 in Figure 5g. In a case of compressive strain (Figure 4a), the *I–V* characteristics were under control of the two components: F_1 has a positive effect on the current, while F_2 has a negative effect on the current. Under an increasing compressive strain, F_1 decreased, while F_2 increased; that is to say the enhancing effect is reduced and the weakening effect is enhanced. As a result, the competition between two effects could lead to a peak value of current as applied strain increased, which is the same situation as type U&D and D&U, as shown in Figure 4a,b.

As a wurzite family material, GaN behaves similar to ZnO, but GaN has a much better chemical stability than ZnO in atmosphere and/or under acid conditions. This provides a possibility to develop GaN-based devices that operate under severe environmental conditions and to make the devices last longer in some corrosive conditions. Also, as the piezotronic effect is proven to be successful in GaN, we can expect to discover more exciting results from other materials of wurtzite crystal structure, such as InN, CdS, and CdSe.

In summary, piezotronic effect on the transport properties of GaN NB has been demonstrated. The *I–V* characteristics of the device were tuned by the piezotronic effect when a compressive/tensile strain was applied on the GaN NB due to the change in Schottky barrier height, with good reproducibility and excellent stability. The configuration was found to play a very important role in this process and different configurations of GaN NB devices leads to different trends of the *I–V* characteristics as well. A theoretical model is proposed to explain such effects on the electrical characterization, especially the SBH of the GaN NB, using the energy band diagram. This effect has potential applications in strain and stress measurements in biomedical sciences, MEMS devices and structure monitoring.

Experimental Section

COMMUNICATION

polydimethylsiloxane (PDMS) was used to package the device, in order to not only enhance the adhesion of the silver paste to the PS substrate, but also prevent the GaN NB from contamination or corrosion by gases or liquid.

Piezotronic Effect on GaN NB Device: To measure the piezotronic effect on the GaN NB devices, one end of the device was fixed tightly on a sample holder with the other end free to be mechanically bent. The tensile and compressive strains were introduced by using a 3D mechanical stage to bend the free end of the device. The performances of the device under different strains were measured using a computer-controlled measurement system.

Acknowledgements

[1] S. Nakamura, M. Senoh, T. Mukai, *Jpn. J. Appl. Phys. 2* **1993**, *32*, L8.
[2] Z. L. Wang, J. H. Song, *Science* **2006**, *312*, 242.
[3] X. D. Wang, J. H. Song, J. Liu, Z. L. Wang, *Science* **2007**, *316*, 102.
[4] a) C. Xu, C. F. Pan, Y. Liu, Z. L. Wang, *Nano Energy* **2012**, *1*, 259; b) C. F. Pan, Z. T. Li, W. X. Guo, J. Zhu, Z. L. Wang, *Angew. Chem. Int. Ed.* **2011**, *50*, 11192.
[5] X. D. Wang, J. Zhou, J. H. Song, J. Liu, N. S. Xu, Z. L. Wang, *Nano Lett.* **2006**, *6*, 2768.
[6] Z. L. Wang, *Adv. Mater.* **2007**, *19*, 889.
[7] J. H. He, C. L. Hsin, J. Liu, L. J. Chen, Z. L. Wang, *Adv. Mater.* **2007**, *19*, 781.
[8] C. S. Lao, Q. Kuang, Z. L. Wang, M. C. Park, Y. L. Deng, *Appl. Phys. Lett.* **2007**, *90*, 262107.
[9] a) C. T. Huang, J. H. Song, W. F. Lee, Y. Ding, Z. Y. Gao, Y. Hao, L. J. Chen, Z. L. Wang, *J. Am. Chem. Soc.* **2010**, *132*, 4766; b) L. Lin, C. H. Lai, Y. F. Hu, Y. Zhang, X. Wang, C. Xu, R. L. Snyder, L. J. Chen, Z. L. Wang, *Nanotechnology* **2011**, *22*, 475401.
[10] H. F. Liu, W. Liu, S. J. Chua, D. Z. Chi, *Nano Energy* **2012**, *1*, 316.
[11] a) Z. Y. Zhang, C. H. Jin, X. L. Liang, Q. Chen, L. M. Peng, *Appl. Phys. Lett.* **2006**, *88*, 073102; b) Z. Y. Zhang, K. Yao, Y. Liu, C. H. Jin, X. L. Liang, Q. Chen, L. M. Peng, *Adv. Funct. Mater.* **2007**, *17*, 2478.
[12] J. L. Freeouf, J. M. Woodall, *Appl. Phys. Lett.* **1981**, *39*, 727.
[13] Y. Liu, Z. Y. Zhang, Y. F. Hu, C. H. Jin, L. M. Peng, *J. Nanosci. Nanotechnol.* **2008**, *8*, 252.
[14] J. Zhou, Y. D. Gu, P. Fei, W. J. Mai, Y. F. Gao, R. S. Yang, G. Bao, Z. L. Wang, *Nano Lett.* **2008**, *8*, 3035.
[15] Y. Liu, M. Z. Kauser, M. I. Nathan, P. P. Ruden, S. Dogan, H. Morkoc, S. S. Park, K. Y. Lee, *Appl. Phys. Lett.* **2004**, *84*, 2112.
[16] a) F. Litimein, B. Bouhafs, Z. Dridi, P. Ruterana, *New J. Phys.* **2002**, *4*, 64; b) Y. F. Li, B. Yao, Y. M. Lu, Z. P. Wei, Y. Q. Gai, C. J. Zheng, Z. Z. Zhang, B. H. Li, D. Z. Shen, X. W. Fan, Z. K. Tang, *Appl. Phys. Lett.* **2007**, *91*, 021915.
[17] Z. L. Wang, *J. Phys. Chem. Lett.* **2010**, *1*, 1388.
[18] Y. Liu, M. Z. Kauser, D. D. Schroepfer, P. P. Ruden, J. Xie, Y. T. Moon, N. Onojima, H. Morkoc, K. A. Son, M. I. Nathan, *J. Appl. Phys.* **2006**, *99*, 113706.
[19] Z. L. Wang, *Adv. Mater.* **2012**, DOI: 10.1002/adma.201104365.